

X-ray luminous galaxies II. Chandra and XMM-Newton Observations of the 'composite' galaxy IRAS20051-1117

I. Georgantopoulos¹ I. Papadakis² A. Zezas³ M. J. Ward⁴

ABSTRACT

We present *Chandra* and *XMM-Newton* observations of the composite star-forming/Seyfert galaxy IRAS20051-1117. The X-ray imaging and spectral properties reveal the presence of an active nucleus. The *Chandra* image shows a strong nuclear point source ($L(2 - 10\text{keV}) \sim 4 \times 10^{42} \text{erg s}^{-1}$). The nuclear X-ray source coincides with a bright, also un-resolved, UV source which appears in the *XMM-Newton* Optical Monitor images. The *XMM-Newton* and *Chandra* spectrum is well represented by a power-law with a photon index of $\Gamma \sim 1.7 - 1.9$ and a thermal component with a temperature of $\sim 0.2 \text{ keV}$. We also detect an Fe line at 6.4 keV with an equivalent width of $\sim 0.3 \text{ keV}$, typical of the iron lines that have been detected in the X-ray spectra of “classical” AGN. We find no evidence for short-term variability in the X-ray light curves, while we detect no variations between the *XMM-Newton* and *Chandra* observations which are separated by about 20 days. Optical spectroscopic observations which were performed ~ 2.5 months after the *XMM-Newton* observation show that the optical spectrum is dominated by a star-forming galaxy component, although a weak broad $H\alpha$ component is present, in agreement with the results from past observations. The lack of strong AGN signatures in the optical spectrum of the source can be explained by the dilution of the nuclear AGN emission by the nuclear star-forming component and the strong emission of the underlying, bright host galaxy.

Subject headings: galaxies: individual (IRAS20051-1117) — galaxies: nuclei — galaxies: active — quasars: general

¹Institute of Astronomy & Astrophysics, National Observatory of Athens, Palaia Penteli, 15236, Athens, Greece

²Physics Department, University of Crete, 71003, Heraklion, Greece

³Harvard-Smithsonian Center for Astrophysics, 60 Garden Street, Cambridge, MA02138

⁴X-ray Astronomy Group, Department of Physics & Astronomy, University of Leicester, LE1 7RH, UK

1. Introduction

Chandra and *XMM-Newton* surveys revealed the presence of a large population of ‘optically inactive’ or ‘passive’ galaxies (Mushotzky et al. 2000, Severgnini et al. 2003, Alexander et al. 2003, Green et al. 2004), confirming previous findings by *ROSAT* (Griffiths et al. 1995, Boyle et al. 1995, McHardy et al. 1998). The optical spectra of these galaxies do not show evidence for either broad or high excitation lines (e.g. Barger et al. 2001). However, in most cases the X-ray luminosities observed are in excess of $L_x \sim 10^{42} \text{erg s}^{-1}$ which is considered as the upper limit for the X-ray emission of bona-fide star-forming galaxies (e.g. Zezas, Georgantopoulos & Ward 1998, Moran et al. 1999) suggesting the presence of active nuclei. It is possible that these galaxies represent a mixed class of objects. In the case of ‘Fiole P3’, which is probably the most well studied case of the ‘passive’ galaxies, Comastri et al. (2002) find that it is most likely associated with an obscured AGN. Severgnini et al. (2003) find instead that a number of galaxies detected in their *XMM-Newton* survey present X-ray spectra with no evidence for absorption. The dichotomy between the optical and X-ray classification could then be explained if the galaxy light dilutes the weak nuclear component (see also Moran et al. 2002, Georgantopoulos et al. 2003 for further examples of such objects).

The ‘optically inactive’ galaxies bear many similarities to the ‘composite’ class of objects discovered by Veron et al. (1981) and further discussed by Moran et al. (1996). The diagnostic emission line diagrams of Veilleux et al. (1995) classify these as star-forming galaxies. Yet, their X-ray luminosities usually exceed $10^{42} \text{erg s}^{-1}$ (Moran et al. 1996); moreover, a fraction of the ‘composites’ present weak H_α broad wings. *Chandra* observations of the ‘composite’ IRAS00317-2142 (Georgantopoulos et al. 2003) showed that the X-ray emission of this object is dominated by a variable nuclear point source which presents an unabsorbed X-ray spectrum. Here, we present *XMM-Newton* and *Chandra* observations of IRAS20051-1117. This is one of the most luminous ‘composite’ objects in the Moran et al. (1996) sample, with a high, soft X-ray luminosity (in excess of $10^{42} \text{erg s}^{-1}$) at a redshift of $z \approx 0.0315$. The diagnostic emission line ratios ($H_\alpha/[NII]$ versus $H_\beta/[OIII]$) classify it as a star-forming galaxy (Moran et al. 1996). Nevertheless, its high X-ray luminosity as well as a faint broad H_α wing would classify this as an AGN. The excellent spatial resolution of *Chandra* combined with the high effective area and good energy resolution of the *XMM-Newton* mission can be used to unveil the nature of the AGN which is hosted in this galaxy. Throughout this paper, we adopt a Hubble constant of $H_0 = 65 \text{km s}^{-1} \text{Mpc}^{-1}$.

2. Observations and Data Reduction

2.1. Chandra

IRAS20051-1117 was observed using the Advanced CCD Imaging Spectrometer, ACIS-S, onboard *Chandra* (Weisskopf et al. 1996). The observation date was 20 April 2002 (Sequence Number 700383). We use the cleaned event file provided by the standard pipeline processing having an exposure time of 20.1 ksec. Only Grade 0,2,3,4 and 6 events are used in the analysis. The whole galaxy falls on only one chip (S3). Charge Transfer Inefficiency (CTI) problems do not affect our observations as S3 is back-illuminated chip. Each CCD chip subtends an 8.3 arcmin square on the sky while the pixel size is $0.5''$. The spatial resolution on-axis is $0.5''$ FWHM. The ACIS-S spectral resolution is ~ 100 eV (FWHM) at 1.5 keV. We observed in 1/4-subarray mode in order to minimize pile-up problems; in this mode the size of the chip is reduced effectively to about 2×8 arcmin. We obtain about 7000 counts in the total 0.3-8 keV band, after background subtraction, corresponding to a count rate of 0.35 cts s^{-1} . Then, the *PIMMS* software estimates a pile-up fraction of less than 10%. Images, spectra, ancillary files, response matrices, and lightcurves have been created using the *CIAO* v2.2 software. We use a $2''$ radius extraction region in order to produce both the spectral files and the lightcurves. We take into account the degradation of the ACIS quantum efficiency in low energies, due to molecular contamination, by using the *ACISABS* model in the spectral fitting¹. The imaging analysis was performed using the *SHERPA* software.

2.2. XMM-Newton

The *XMM-Newton* data were obtained in 01 April 2002 as part of the Guest Observer Programme AO-1. The EPIC (European Photon Imaging Camera; Strüder et al. 2001 and Turner et al. 2001) cameras were operated in full frame mode with the thin filter applied. The data have been cleaned and processed in the standard pipeline mode using the Science Analysis Software (SAS). The event files for the PN and the two MOS detectors were produced using the standard reduction pipeline (Watson et al. 2001). The event files were screened for high particle background periods resulting in a good time interval of about 5.5 ksec for both MOS and PN. Events corresponding to patterns 0–4 and 0–12 have been included in the analysis of the PN and MOS data respectively. We obtain about 5500 and 3500 background subtracted counts in the PN and the combined MOS respectively. The resulting count rates are ≈ 1 and 0.7 cts s^{-1} respectively. We use a 4 pixel ($\sim 16''$) radius

¹<http://asc.harvard.edu/cal/Acis/Cal.prods/qeDeg>

extraction region, in order to obtain the spectrum (and the lightcurve) of our source. We obtain the background from a region from the same CCD chip with an area about 10 times larger than the source extraction region. We create the auxiliary files for the PN and MOS using the SAS task ARFGEN to take into account both instrumental effects (e.g. quantum efficiency, telescope effective area, filter transmission) and the fraction of light falling outside the extraction radius. The spectral response files are created using the task RMFGEN.

Finally, during the *XMM-Newton* observation, the OM (Optical Monitor) was operated in Imaging mode. The source was observed with the B, UVW1 (i.e. U) and UVW2 filters. The total exposure time was 4, 5 and 6 ksec respectively. In the subsequent analysis we use the processed, standard pipeline mode data (which were reduced using SAS version 5.3.2).

3. Data Analysis

3.1. Imaging

In Fig. 1 we plot the *Chandra* X-ray contours in the total band (0.3-8 keV) overlayed on the *XMM-Newton* OM (Optical Monitor) image in the U (UVW1, 2900 Å) filter. All the X-ray emission emanates from the source coinciding with the optical nucleus. The coordinates of the X-ray source are $\alpha = 20^h07^m51.3s$, $\delta = -11^\circ08'33s$ (J2000); note that the *IRAS* name for this object refers to B1950.

We have fitted the two-dimensional spatial profile of the *Chandra* source with the SHERPA software. Fitting a Gaussian profile, we obtain a FWHM of 1.78 ± 0.02 pixels. Given that the nominal Point Spread Function (PSF) is undersampled by the pixels of the ACIS camera ($\text{FWHM}_{PSF} \sim 0.5''$ at 1.5 keV, compared to a pixel size of $0.49''$) we consider the probability of any extension marginal. Indeed, the Gaussian fit to the Point Spread Function generated with the CIAO MKPSF task gives a comparable FWHM ($\approx 1.5 \pm 0.02$ pixels).

Fig. 1 shows that the central UV-bright source in IRAS20051-1117 is surrounded by some faint nebulosity which is associated with the galaxy. The nuclear source appears to be point-like in the UV. In order to investigate this issue further, we co-added the 5 UVW1 and UVW2 images to create a single image. Using IRAF, we fitted the one-dimensional radial profile of the central source in both filters with a Gaussian. The FWHM of the Gaussian profile is $\sim 2.5''$ and $\sim 1.8''$ in the case of the UVW1 and UVW2 images, respectively. The profile of the UVW1 source appears to be slightly larger than the width of the nominal PSF for this filter ($1.7''$). The FWHM of the UVW2 source is identical to the PSF width for this filter ($1.8''$). As the contribution of the underlying galaxy is much more pronounced in the

UVW1 image, our results imply that, just like with the X-ray source, the UV source is not resolved either, its size being equal to or smaller than $\sim 2''$ which corresponds to ~ 1.4 kpc.

3.2. Timing

Fig. 2 (upper panel) shows the background subtracted PN and MOS light curves for IRAS20051-1117 in the 0.3 - 8 keV band (open squares, filled and open circles for PN, MOS-1 and MOS-2 light curves, respectively). The time bin size was set to 200 sec. All cameras were switched on about the same time, however there are a few gaps of duration $\sim 20 - 800$ sec in all light curves, due to the rejection of periods with high particle background. The light curves appear to be flat, with no significant variations above the instrumental noise. Using the χ^2 test, we find that the light curves are consistent with the hypothesis of a constant flux. This is true even when we consider the combined, background subtracted PN and MOS light curves. The *Chandra* 0.3-8 keV light curve does not show any significant, intrinsic variations either (Fig. 2, lower panel). We conclude that IRAS20051-1117 does not show any significant variations on time scales smaller than ~ 10 ksec.

Next, we examine whether there is any evidence for long term variability. Using the best fit power-law spectrum derived from the PN data ($\Gamma = 1.94$ see section 3.3 below) we derive a 2-10 keV flux of $1.5 \pm 0.025 \times 10^{-12}$ and $1.5 \pm 0.020 \times 10^{-12}$ erg cm $^{-2}$ s $^{-1}$ from the *XMM-Newton* (PN) and *Chandra* data respectively, suggesting that the nucleus presents no variability. However, as the *Chandra* and *XMM-Newton* observations are separated by a small interval of about 3 weeks, we have also checked whether other X-ray missions have obtained in the past observations of our object. *ROSAT* (PSPC) has observed IRAS20051-1117 in the second semester of 1990 during the ROSAT-All-Sky-Survey (exposure time 411s). The count rate of 0.07 ± 0.01 (0.1-2.4 keV) translates to an absorbed flux of $8.4 \pm 1.2 \times 10^{-13}$ erg cm $^{-2}$ s $^{-1}$ in the 0.3-2 keV band (using the best-fit PN model). This is consistent with the observed *XMM-Newton* and *Chandra* flux in the same energy band ($\sim 1 \times 10^{-12}$ erg cm $^{-2}$ s $^{-1}$), within $\sim 1.3\sigma$.

3.3. The X-ray spectra

The spectra are grouped, using the FTOOL GRPPHA task to give a minimum of 20 (15) counts per bin for *XMM-Newton* (*Chandra*) to ensure that Gaussian statistics apply. The quoted errors to the best fitting spectral parameters correspond to the 90 % confidence level for one interesting parameter. In order to assess the significance of new parameters added

to a model we have adopted the 95 % confidence level, using the F -test for additional terms. We discard data below 0.3 and above 8 keV due to the low response of the ACIS-S, PN and MOS cameras. We fit the data using the XSPEC v11.2 software package. The spectral fits are presented separately for the *Chandra* and the *XMM-Newton* data.

a) The *XMM-Newton* spectral fits. We first fit the PN data using a single power-law model absorbed by two columns: one fixed to the Galactic ($N_H \approx 7 \times 10^{20}$ Dickey & Lockman 1990) and one intrinsic which is left free to vary. We find that this model provides a relatively poor fit ($\chi^2 = 268.7/190$) to the data. The power-law has the 'canonical' slope, $\Gamma = 1.92_{-0.07}^{+0.08}$, while the 90 % upper limit of the intrinsic column is $< 1 \times 10^{20} \text{ cm}^{-2}$.

The addition of a narrow line ($\sigma < 0.01$ keV i.e. smaller than the CCD's spectral resolution at these energies) at 6.4 keV (rest-frame) results in a better fit. We find $\Delta\chi^2 = 10.3$ for one additional parameter (the normalization of the Gaussian line) which is statistically significant at the > 99 % confidence level. The equivalent width of the Fe line is 360_{-170}^{+174} eV consistent with that predicted for unobscured AGN (e.g. Page et al. 2004) with comparable X-ray luminosity. The spectral results are presented in table 1. In Fig. 3 (upper panel) we plot the model fit to the data together with the data to model ratio. Inspection of the residuals suggests the possibility that some additional lines are present: e.g. Fe at 6.96 keV, Ca at 3.9 keV, Si at 1.9 keV (rest-frame). However, only the first line (Fe) is detected at over the 95 per cent confidence level. The resulting equivalent width is 371_{-206}^{+263} eV. The presence of residuals at low energies prompted us to test for the presence of thermal emission. The inclusion of a Raymond-Smith spectrum (abundance fixed at $Z=0.3$) results in a significantly better fit $\chi^2 \approx 233.3/186$. The temperature of this component ($kT = 0.20_{-0.02}^{+0.06}$ keV) is consistent with the properties of hot gas emission in nearby star-forming galaxies (e.g. Stevens et al. 2003). Its luminosity is $L_{0.3-8\text{keV}} \sim 2 \times 10^{41} \text{ erg s}^{-1}$.

The MOS data are fitted with the normalizations untied between the MOS1 and MOS2 detectors. The single power-law model gives a good fit ($\chi^2 = 128.5/121$) with a photon index $\Gamma = 2.0_{-0.09}^{+0.11}$ and an intrinsic column density of $5_{-1}^{+2} \times 10^{20} \text{ cm}^{-2}$. The low effective area of the MOS detectors at high energies, hampers us from placing any constraints on the properties of the Fe lines above 6 keV. The addition of an Fe line results in the reduction of the χ^2 by only 0.1. Moreover, the inclusion of a Raymond-Smith component is not statistically significant. Finally, a joint fit to the PN and MOS data (with the normalizations between the 3 detectors untied) yields $\Gamma = 1.96_{-0.06}^{+0.06}$, $N_H = 2_{-1}^{+1} \times 10^{20} \text{ cm}^{-2}$ ($\chi^2 = 381.9/313$). The normalizations between the 2 MOS instruments agree within 5% while those between MOS and PN within 20 %. The inclusion of the two Fe lines and the Raymond-Smith component is statistically significant yielding $\Gamma = 1.96_{-0.06}^{+0.08}$, $N_H = 3_{-1}^{+2} \times 10^{20} \text{ cm}^{-2}$ ($\chi^2 = 347.9/307$).

b) The *Chandra* spectral fits. A single power-law fit to the data gives $\Gamma = 1.79 \pm 0.04$

with a negligible intrinsic column density of $0.1 \times 10^{20} \text{ cm}^{-2}$ ($\chi^2_\nu = 290.5/202$). The above values are in reasonable agreement with those derived from the PN. The addition of an Fe line at 6.4 keV reduces the χ^2 by 6.9 which is statistically significant at the $\approx 97\%$ confidence level. The equivalent width of the line is $250 \pm 155 \text{ eV}$, comparable to the value found from the model fitting of the PN data. The *Chandra* spectrum is plotted in Fig. 3 (lower panel) together with the data to model ratio. Finally, the addition of a Raymond-Smith component results in the improvement of the fit ($\chi^2 \approx 246.3/199$). The temperature of the Raymond-Smith component is $0.22 \pm 0.03 \text{ keV}$ in good agreement with *XMM-Newton* while the power-law photon index is flatter (1.67 ± 0.05). The reduction of the χ^2 , when the thermal component is added, may suggest the presence of a compact nuclear star-forming region. Alternatively, it is possible that many *photo-ionization* line residuals at soft energies are reduced with the inclusion of the above component.

3.4. Optical Observations

Optical spectroscopic observations were made with the 1.3 m telescope at Skinakas Observatory (Crete, Greece) on 2002 June 21. The f/7.7 Ritchey-Cretien telescope was equipped with a 1024×1024 SITe chip plus a $651 \text{ lines mm}^{-1}$ grating, giving a dispersion of $\sim 3.3 \text{ \AA/pix}$. We used a $2''$ slit which corresponds to a physical size of 1.4 kpc at the redshift of our object. The spectra span the $4300 - 7400 \text{ \AA}$ range, at a resolution of $\sim 7.0 \text{ \AA FWHM}$. The total integration time was 1.5 hrs.

The optical spectrum of the source is shown in Fig. 4. It is similar to the spectrum presented by Moran et al. (1996). We detect strong $\text{H}\alpha$, $[\text{N II}]$, $[\text{S II}]$ and $[\text{O III}]$ and much weaker $\text{H}\beta$ (narrow) and $[\text{O I}]$ lines. $\text{H}\alpha$ has a broad component with a width of $\sim 3800 \text{ km/sec}$. Our measurements of the galaxy emission line flux ratios are as follows: $[\text{O III}]/\text{H}\beta(\text{narrow})=1.1$, $[\text{O I}]/\text{H}\alpha(\text{narrow})=0.019$, $\text{H}\alpha(\text{narrow})/\text{H}\beta(\text{narrow})=2.65$, $\text{H}\alpha(\text{broad})/\text{H}\beta(\text{narrow})=3.69$, $[\text{NII}]/\text{H}\alpha(\text{narrow})=0.59$, and $[\text{SII}]/\text{H}\alpha(\text{narrow})=0.33$. The ratios for the bright lines are slightly smaller (by a factor of $\sim 1.5 - 2.5$) than the respective values listed in Table 3 of Moran et al. (1996). These differences are not highly significant, specially if one considers the fact that different ratio values can be obtained if the seeing and/or extraction apertures differ since in this case different amounts of the host galaxy are included in the aperture. Furthermore, for the fainter lines ($\text{H}\beta$ and $[\text{O I}]$) our measurements are quite uncertain because of the poor quality of the data (the overall signal-to-noise of the optical spectrum is ~ 5). Despite these small differences, the position of the source on the standard emission line diagnostic diagrams (e.g. Veilleux et al. 1995) confirms that this object lies between the HII region and AGN loci.

From the ratio between $H\alpha(\text{narrow})$ and $H\beta$, we calculate a reddening of $E(B - V) = -0.08$ and $E(B - V) = 0.002$ for an AGN and an HII region intrinsic continuum respectively. These correspond to an equivalent HI column density of $4 \times 10^{20} \text{ cm}^{-2}$ and $1 \times 10^{19} \text{ cm}^{-2}$, assuming Galactic gas-to-dust ratio (Bohlin et al 1978). As the reddening mentioned above refers to the sum of the Galactic and intrinsic extinction, this result agrees well with the result of no intrinsic absorption as derived from the model fitting to the EPIC PN X-ray spectrum.

3.5. The spectral energy distribution (SED)

The availability of simultaneous UV (OM) and X-ray (EPIC-PN) observations by *XMM-Newton* gives us the opportunity to investigate the UV/X-ray energy distribution of the source. For the OM data, we first estimated the mean count rate of the individual images (as formed by summing the counts within a $16''$ diameter aperture centered on the nucleus). We have not corrected for the contribution of the underlying galaxy, which increases towards larger wavelengths (reaching $\sim 30\%$ in the B filter). We transformed the average count rates to magnitudes using the appropriate 'Zeropoint magnitude' value for each filter (as listed in the *XMM-Newton* users manual). For the reddening correction we assumed no intrinsic absorption, and adopted the Galactic extinction value, $A_V \approx 0.4$, of Schlegel et al. (1998). Using the A_λ versus λ relationship of Cardelli et al. (1989) for $R_V = 3.1$, we then found A_λ at $\lambda = 4400, 2900$, and 2150 \AA (i.e. the wavelengths at which the response of the B, UVW1, and UVW2 filters peaks).

The UV/X-ray energy distribution is shown in Fig. 5, plotted as νf_ν versus ν . For the X-ray data we used the best fitting power law model to the *XMM-Newton* EPIC-PN spectrum (the long dashed lines represent power law models with slopes equal to the best fitting slope $\pm 1\sigma$ confidence limit values). In the UV band, the ratio $\nu f_{UVW2}/\nu f_{UVW1}$ is comparable with the ratio of the respective frequencies. This result implies that $\nu f_{nu} \propto \nu$, in agreement with the trend shown by the mean energy distribution of radio-quiet AGN in the same energy band (e.g. Elvis et al. 1994). Using the data shown in Fig. 5, we find that the monochromatic X-ray (2 keV) to UV (2500 \AA) luminosity ratio for IRAS20051-1117 is $\alpha_{ox} = 1.42$. This is consistent with the average value of ~ 1.6 for radio-quiet AGN (Stocke et al. 1991).

The OM, B band measurement indicates that the SED rises towards longer wavelengths. This trend is caused by the fact the host galaxy's underlying emission in this band is quite stronger than the emission in the UV wavelengths. A quasi-simultaneous flux measurement at longer wavelengths is also possible based on the optical spectrum of the source. Since

this spectrum was taken only ~ 2.5 months after the *XMM-Newton* observation we used it in order to estimate a “V” band measurement. To that aim, we computed the average flux in the $5400 - 5600 \text{ \AA}$ band (observer’s frame), which is free of lines, and we dereddened it adopting $A_V \approx 0.4$, as before. Interestingly, although the optical spectrum was taken using a $2''$ wide slit (i.e. significantly smaller than the aperture size that we use for the OM photometry), the V band flux that we measure is larger than that in the B band. This result gives further support to the idea that the SED rises towards longer wavelengths.

This trend is confirmed when we consider the near and far infrared measurements of the source. For the J, H, and K bands we used the 2MASS measurements (in a aperture of size $14'' \times 14''$). For the far-infrared band we used the IRAS measurements at 25, 60, and 100 microns, from the IRAS faint source catalogue. Although the near-infrared and UV flux measurements are taken from apertures which have almost identical areas, the strong rise from optical to near-infrared wavelengths shown in Fig. 5 shows that the energy release in the near-infrared band is significantly larger than that released in the UV band. In IRAS20051-1117, it is the near-infrared/optical which rises above its UV continuum, and not the other way around, as it is observed in most galaxies with a strong active nucleus.

Apart from the strong contribution of the galaxy stellar population in the near-infrared bands, the strong far infrared emission is indicative of the presence of a significant star formation rate (SFR). For example, using the relation between logarithm of SFR and logarithm of galaxy luminosity at 100 microns of Misiriotis et al. (2004), we find an overall SFR of $\sim 32 \text{ M}_\odot \text{ yr}^{-1}$. This is typical of bright IRAS galaxies, but much smaller than SFR in starburst galaxies.

4. Discussion

In this work, we present the results from X-ray and optical observations of IRAS20051-1117. The *Chandra* and *XMM-Newton* OM images reveal the presense of a strong, UV and X-ray bright nuclear source, which is un-resolved in both cases. The FWHM of the X-ray source is $\sim 1''$, which corresponds to a region of size $\sim 0.7 \text{ kpc}$ at the distance of the object. The X-ray spectrum of the nucleus is very similar to the typical AGN spectra: a power-law model fitting to the EPIC-PN spectrum shows the canonical spectral slope of $\Gamma \sim 1.9$, and reveals the presence of an iron line at 6.4 keV . The equivalent width of the line is consistent with that of unobscured AGN of comparable luminosity (e.g. Page et al. 2004). We also detect evidence for the presence of ionized material in the vicinity of the nucleus, as indicated by the presence in the spectrum of a line at 6.96 keV which we interpret as emission from ionized iron. Thermal emission with a low temperature (0.2 keV) is present

in both the *XMM-Newton* and the *Chandra* spectrum.

The presence of a strong, point-like nuclear UV and X-ray source, with an X-ray spectrum typical of AGN, shows conclusively that the intense X-ray emission of IRAS20051-1117 is produced by a Seyfert-like nucleus in the center of this galaxy. This is further supported by the fact that the UV/X-ray energy spectral distribution of this object is very similar to the SEDs of AGN in the same energy band. In particular, the “X-ray loudness” of this object, $\alpha_{\text{ox}} \approx 1.4$, is consistent with the average X-ray/UV luminosity ratio found for radio-quiet AGNs.

However, optical observations that were performed only 2.5 months after the *XMM-Newton* observations of IRAS20051-1117, reveal an optical spectrum very similar to the spectrum presented by Moran et al. (1996). The emission-line flux ratios places this galaxy on the boundary between regions ordinarily populated by HII and Seyfert galaxies. Although there are signs of Seyfert activity as well (such as the presence of a weak, broad component of the $H\alpha$ line), the optical spectrum is dominated by characteristics of HII galaxies. Moran et al. (1996) have suggested that “obscuration” effects may be responsible for the optical spectra of “composite” galaxies. However, both the *XMM-Newton* and *Chandra* observations of IRAS20051-1117 show no sign of any intrinsic absorption in this galaxy. There is a possibility that the X-ray nucleus is totally obscured (Compton-thick) in which case we are viewing the reflected component in the backside of the torus. The lack of variability between the *XMM-Newton* and the *Chandra* epochs (as well as the *ROSAT* epoch) could in principle favor such an interpretation. Nevertheless, the moderate equivalent width of the Fe line, combined with the steep X-ray spectrum (see e.g. Matt et al. 1996) argue against the reflection component scenario. The detection of a strong nuclear UV source and of a broad $H\alpha$ in the low signal-to-noise optical spectrum further support the hypothesis that we are viewing directly the Seyfert nucleus. Ward et al. (1988) have noted the presence of a tight correlation between the broad $H\alpha$ and the hard X-ray (2-10 keV) luminosity in unobscured AGN. Our object has an $H\alpha$ luminosity of $7 \times 10^{40} \text{ erg s}^{-1}$ (Moran et al. 1996) which translates to a predicted 2-10 keV X-ray luminosity of $4 \times 10^{42} \text{ erg s}^{-1}$, in excellent agreement with the *Chandra* and *XMM-Newton* observations, further suggesting that the Broad Line Region is not obscured in our object.

One possibility that could explain the optical spectral properties of IRAS20051-1117 is that it hosts a non-standard broad line region. For some reason, much less gas in the central source of this object is illuminated by the ionizing continuum, than in a typical AGN. Or perhaps, the broad line region may even be absent in this source. A third possibility though, and perhaps a more realistic one, is that the AGN optical signature is not evident in this source because of the presence of a starburst component (Moran et al., 1996) and because

it is partially diluted by the presence of the strong optical continuum of the host galaxy. IRAS20051-1117 is a luminous spiral galaxy, as its optical/near-infrared excess emission in the overall SED implies (Fig. 5). Its total K-band magnitude is 11.28 (2MASS survey) which translates to an absolute magnitude of $M_K = -24.5$. Using an average colour of $R-K = 2.36$, appropriate for spiral galaxies of morphological type $0 \leq T \leq 6$ (de Jong, 1996), we find $M_R = -22.14$. Severgnini et al. (2003) estimate that the optical signature of X-ray unabsorbed AGN with X-ray luminosity up to $\sim 10^{43}$ erg s $^{-1}$ (the case of IRAS20051-1117), may be hidden if they are hosted by a galaxy with $M_R \leq -22$. In fact, their calculations indicate that only H α will show clearly the appearance of the central active nucleus, exactly like the case with IRAS20051-1117, as only H α shows clear evidence for a broad component.

Finally, we do not detect any significant variations in both the *Chandra* and *XMM-Newton* light curves. X-ray variability has become one of the defining characteristics of AGN the last years. However, the lack of detection of significant variations is not surprising, given the short duration of the X-ray light curves. For example, the *XMM-Newton* EPIC-PN light curve is less than 10 ksec. For a $\sim 10^{43}$ erg/s source, we expect to measure an “excess variance”, σ_{nxs}^2 (i.e. the variance of a light curve normalized by its mean squared after correcting for the experimental noise) of ~ 0.01 in light curves as long as ~ 1 day (e.g. Nandra et al., 1997). If σ_{nxs}^2 increases proportional to the length of the light curve, then we expect $\sigma_{nxs}^2 \sim 0.0015$ in the case of the present IRAS20051-1117 light curves. However, due to the low count rate, even in the combined EPIC PN and MOS light curve, the uncertainty on the estimation of σ_{nxs}^2 due to the experimental Poisson noise (found using equation 11 of Vaughan et al., 2003) is twice as large as the expected “signal” that we want to detect. Clearly, a longer X-ray light curve is needed in order to detect significant, short term variations in IRAS20051-1117. More surprising is the lack of “long term” variations, when we compare the observed X-ray flux during the *XMM-Newton*, *Chandra* and *ROSAT* observations, which are separated by 3 weeks and 12 years, respectively. Only monitoring X-ray observations over a period of months/years could allow us to investigate the variability behavior of this source.

5. Summary

We present *Chandra* and *XMM-Newton* observations of IRAS20051-1117 one of the ‘composite’ galaxies in the Moran et al. (1996) sample of galaxies. The *Chandra* data show that the X-ray emission comes from a nuclear point-like source with a luminosity of $L(2 - 10\text{keV}) \sim 4 \times 10^{42}$ erg s $^{-1}$. This coincides with a bright, UV nucleus as revealed by the UV imaging performed with the OM on-board *XMM-Newton*. The X-ray spectrum

(*XMM-Newton* and *Chandra*) is represented by a power-law spectrum with a steep photon index $\Gamma \sim 1.7 - 1.9$ and a thermal component with a temperature of ~ 0.2 keV absorbed by a negligible intrinsic column density $< 3 \times 10^{20} \text{ cm}^{-2}$. An Fe line at 6.4 keV is also detected in both the *XMM-Newton* and *Chandra* data with an equivalent width of ~ 300 eV. The above give away the presence of an active nucleus. There is no variability between the *Chandra* and the *XMM-Newton* flux which are separated by a small period of about 3 weeks. Puzzlingly, there is no observed variability in the soft X-ray flux between *XMM-Newton* and *Chandra* and the *ROSAT* observation which are separated by a period of more than 12 years. The marked lack of variability could suggest the presence of a highly obscured (Compton-thick) AGN. However, this possibility is probably ruled out by the moderate equivalent width of the Fe line, the steep X-ray spectrum observed and the ratio of the hard X-ray to the $H\alpha$ luminosity which are typical of unobscured AGN.

The nuclear optical spectrum (using a $2''$ slit which corresponds to a ≈ 1.5 kpc region at the source) obtained 2.5 months after the *XMM-Newton* observation, presents a weak broad $H\alpha$ line. Nevertheless, the optical spectrum is dominated by a strong star-forming component which outshines the AGN signatures. The weakness of the AGN features could be attributed to the dilution of the nuclear AGN emission by the star-forming component and the strong host galaxy optical emission.

IRAS20051-1117 presents many similarities with the luminous X-ray galaxies which have been detected in deep X-ray surveys. Although these are clearly associated with AGN having high X-ray luminosities, their optical spectra show no AGN signatures. The present observations help us to shed light on the properties of such objects and to understand why these fail to reveal strong AGN signatures in the optical band. This work demonstrates in agreement with earlier work (Georgantopoulos et al. 2003, Severgnini et al. 2003) that heavy obscuration may not always be responsible for the discrepancy observed between the X-ray and optical classification.

This work has been supported by the NASA grant G01-2120X. Support is also acknowledged by the grant 'X-ray Astrophysics with ESA's mission XMM' in the framework of the programme 'Excellence in Research' jointly funded by the the European Union and the Greek Ministry of Development. Skinakas Observatory is a collaborative project of the University of Crete, the Foundation for Research and Tecnology-Hellas, and the Max-Planck-Institut für Extraterrestrische Physik. This research has made use of the NASA/IPAC Extragalactic Database (NED) which is operated by the Jet Propulsion Laboratory, California Institute of Technology, under contract with the National Aeronautics and Space Administration.

REFERENCES

- Alexander, D.M. et al. 2003, AJ, 126, 539
- Barger, A.J., Cowie, L.L., Mushotzky, R.F., Richards, E.A., 2001, AJ, 121, 662
- Bohlin, R.C., Savage, B. D., Drake, J.F., 1978, ApJ, 224, 132
- Boyle, B.J., McMahon, R.G., Wilkes, B.J., Elvis, M., 1995, MNRAS, 276, 315
- Cardelli, J.A., Clayton, G.C., Mathis, J.S., 1989, ApJ, 345, 245
- Comastri, A., et al., ApJ, 571, 771
- de Jong, R.S., 1996, A&A, 313, 377
- Dickey, J.M., Lockman, F.J., 1990, ARA&A, 28, 215
- Elvis, M., et al., 1994, ApJS, 95, 1
- Georgantopoulos, I., Zezas, A., Ward, M.J., 2003, ApJ, 584, 129
- Green, P.J. et al. 2004, ApJS, 150, 43
- Griffiths, R.E., Georgantopoulos, I., Boyle, B. J., Stewart, G.C., Shanks, T., della Ceca, R., 1995, MNRAS, 275, 77
- Matt, G., et al. 1996, 281, L69
- McHardy, I.M., et al., 1998, MNRAS, 295, 641
- Misiriotis A., Papadakis I.E., Kylafis N.D., Papamastorakis J., 2004, A&A, 417, 39
- Moran, E.C., Halpern, J.P., Helfand, D.J., 1996, ApJS, 106, 341
- Moran, E.C., Lehnert, M.D., Helfand, D.J., 1999, ApJ, 526, 649
- Moran, E.C., Filippenko, A.V., Chornock, R., 2002, ApJ, 579, L71
- Mushotzky, R.F., Cowie, L.L., Barger, A.J., Arnaud, K. A. 2000, Nature, 404, 459
- Nandra, K., George, I.M., Mushotzky, R.F., Turner, T.J., Yaqoob, T. 1997, ApJ, 476, 70
- Page, K. L., O’Brien, P.T., Reeves, J. N., Turner, M.J.L., 2004, MNRAS, 347, 316
- Schlegel, D.J., Finkbeiner, D.P., Davis, M., 1998, ApJ, 500, 525
- Severgnini, P. et al. 2003, A&A, 406, 483
- Stevens, I.R., Read, A.M., Bravo-Guerrero, J., 2003, MNRAS, 343, L47
- Stocke, J., et al. 1991, ApJS, 76, 813
- Vaughan, S., Edelson, R., Warwick, R.S., Uttley, P., 2003, MNRAS, 345, 1271
- Veilleux S., Kim D.-C., Sanders D.B., Mazzarella J.M., Soifer B.T., 1995, ApJS, 98, 171

- Veron, P., Veron, M.P., Bergeron, J., Zuidervijk, E.J., 1981, A&A, 97, 71
- Ward, M. J., Done, C., Fabian, A.C., Tennant, A.F., Shafer, R.A., 1988, ApJ, 324, 767
- Watson, M.G., 2001, A&A, 365, L51
- Weisskopf, M.C., O’dell, S.L., van Speybroeck, Leon P., 1996, SPIE, 2805, 2
- Zezas, A., Georgantopoulos, I., Ward, M.J., 1998, MNRAS, 301, 915

Table 1: The spectral fits results

	Γ	N_H 10^{20}cm^{-2}	E_1 keV	E_2 keV	kT keV	χ^2/dof
PN	$1.94^{+0.08}_{-0.10}$	4^{+3}_{-2}	6.4	6.96	$0.20^{+0.06}_{-0.02}$	233.3/186
MOS	$2.00^{+0.11}_{-0.09}$	5^{+2}_{-1}	-	-	-	128.5/121
PN+MOS	$1.96^{+0.08}_{-0.06}$	3^{+2}_{-1}	6.4	6.96	$0.24^{+0.06}_{-0.06}$	347.9/307
ACIS-S	$1.67^{+0.05}_{-0.05}$	< 2	6.4	-	$0.22^{+0.03}_{-0.03}$	246.3/199

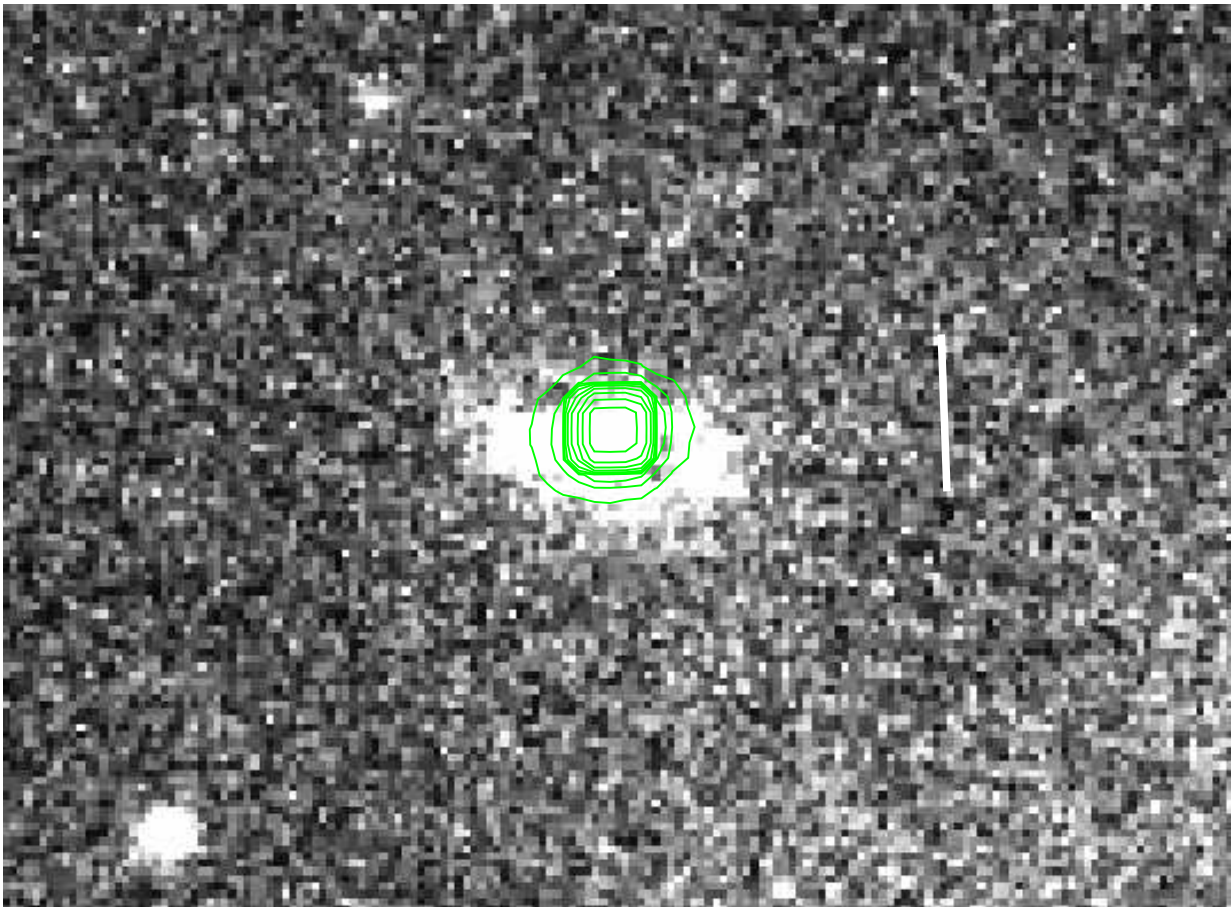


Fig. 1.— The X-ray contours from the 0.3-8 keV *Chandra* image, overlaid on the *XMM-Newton* OM image (U filter). The line corresponds to $10''$.

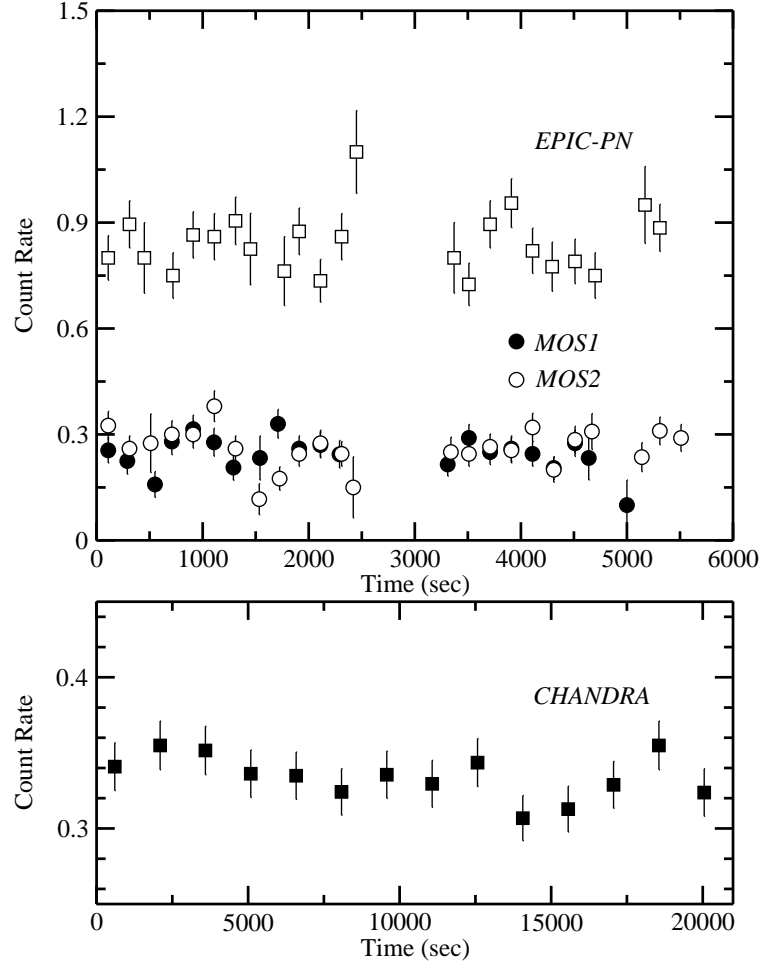


Fig. 2.— Upper panel: *XMM-Newton* EPIC-PN, MOS-1 and MOS-2, background subtracted, 0.3 – 8 keV light curves of IRAS20051-1117, grouped in 200 s bins (open squares, filled and open circles respectively). Time is counted from the start of the PN observation (for clarity reasons the points have been sifted by +50 s on the time axis). Lower panel: *Chandra*, background subtracted, 0.3 – 8 keV light curves of IRAS20051-1117, grouped in 1500 s bins. Time is counted from the start of the *Chandra* observation (for clarity reasons the points have been sifted by +300 s on the time axis).

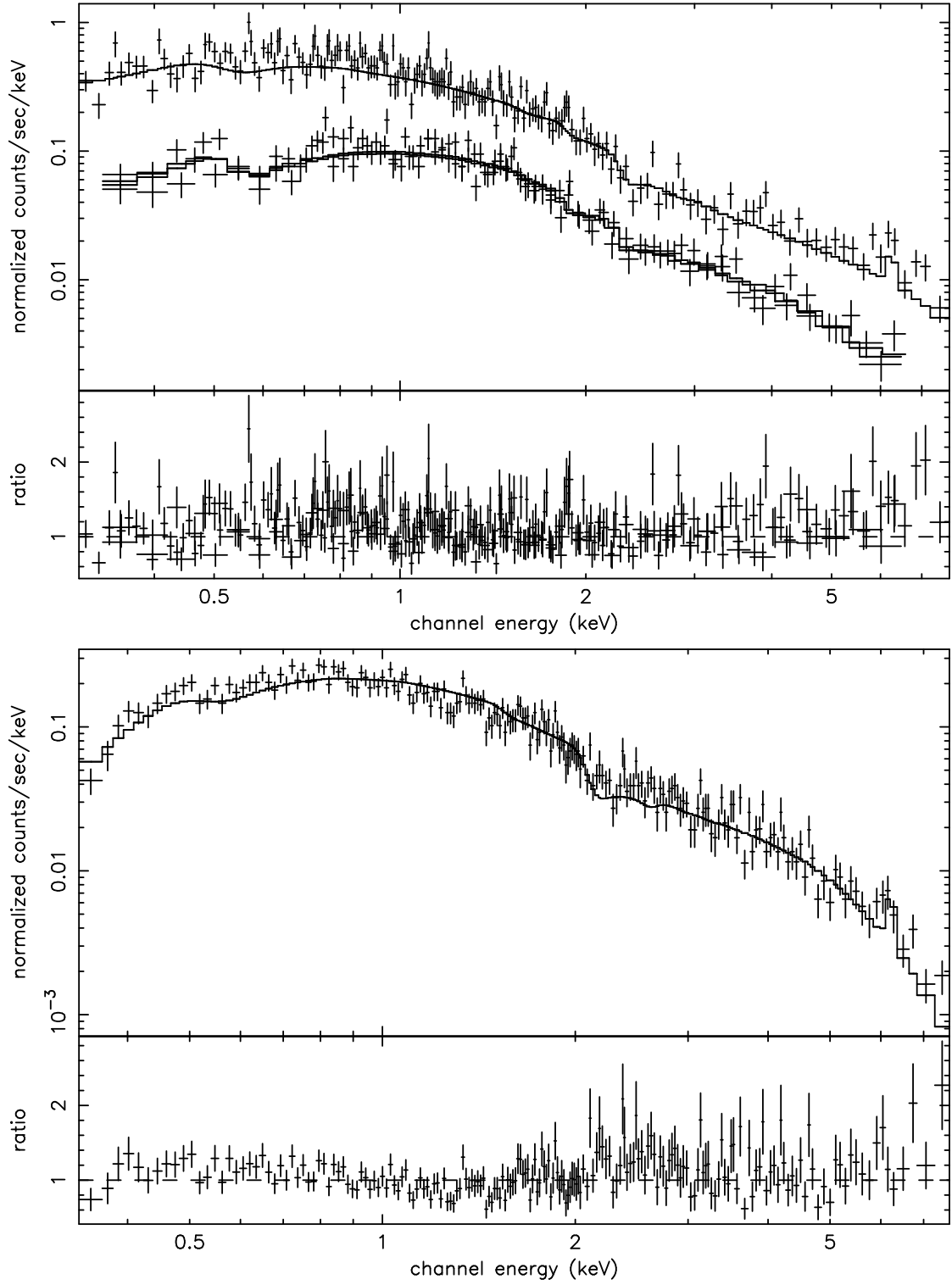


Fig. 3.— The *XMM-Newton* PN (upper panel) and *Chandra* (lower panel) spectra plotted together with a model fit consisting of a power-law plus a 6.4 keV Gaussian line, absorbed by the Galactic and an intrinsic column density. The data to model ratios are given as well.

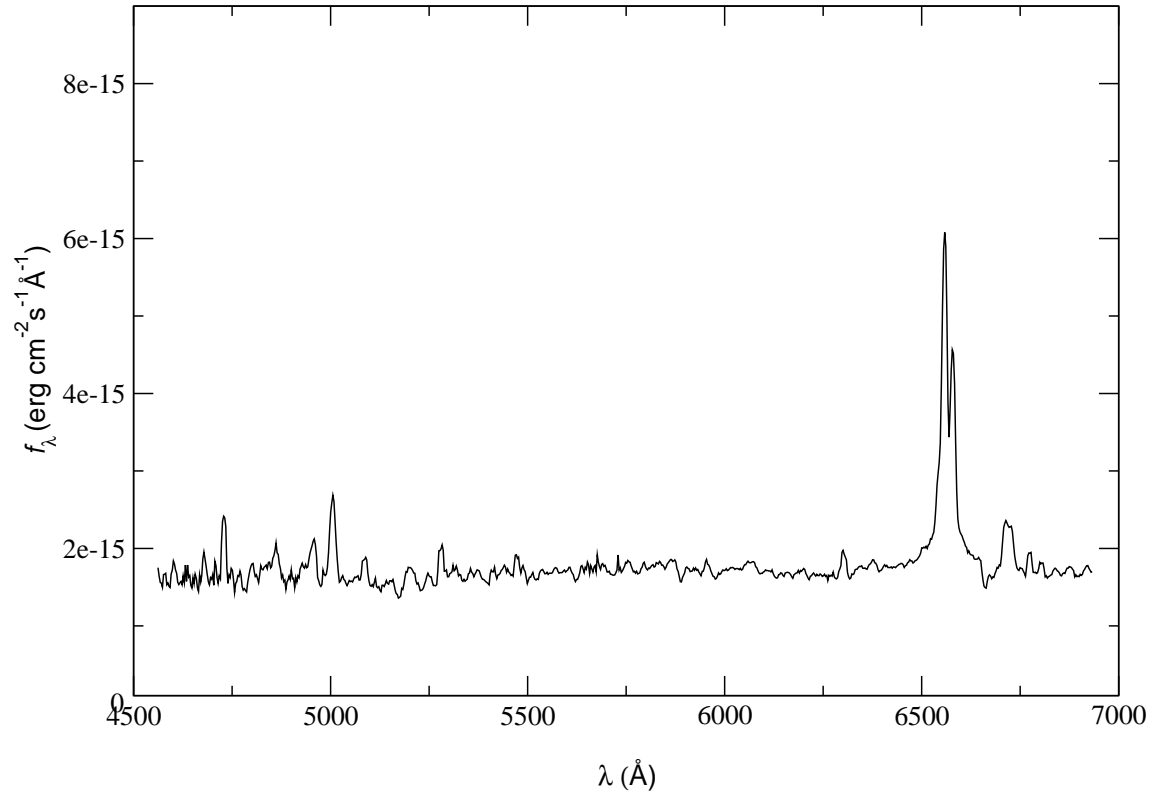


Fig. 4.— The optical spectrum of IRAS20051-1117 taken in June 2002, from Skinakas observatory. The spectrum, plotted as flux per unit wavelength interval, has been shifted to rest frame.

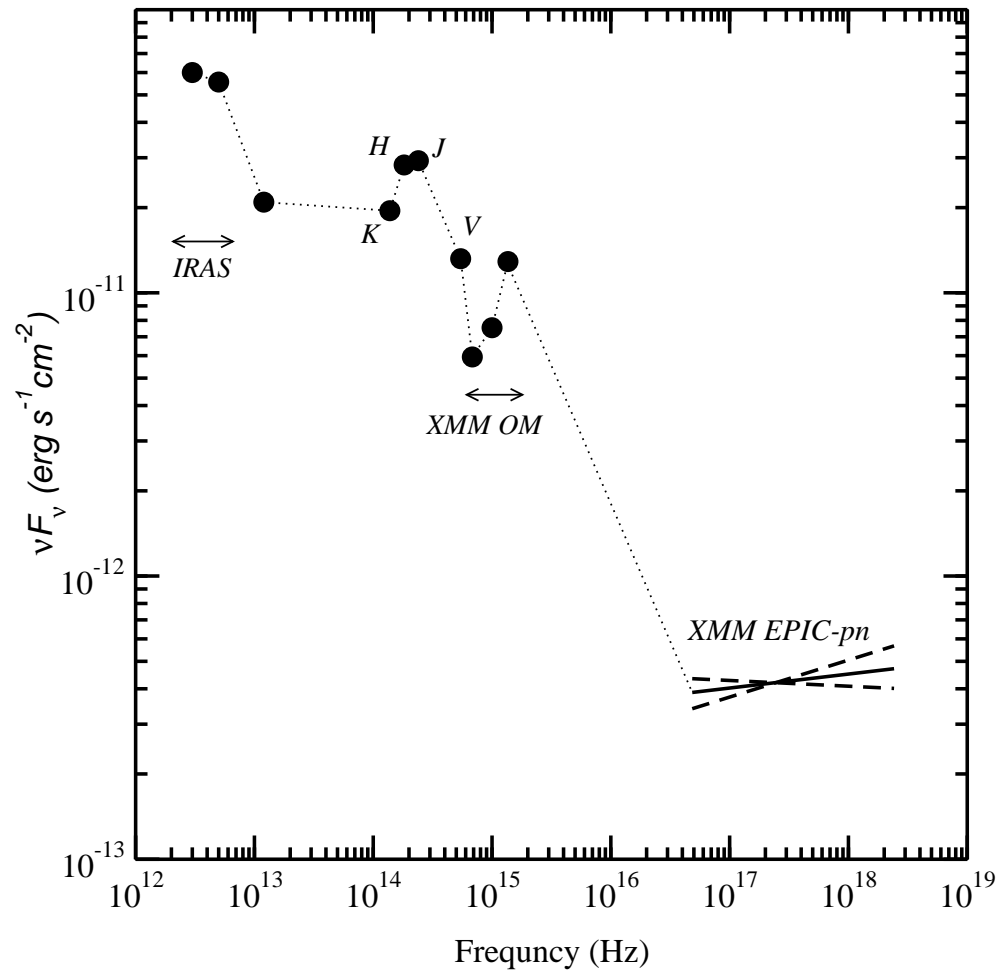


Fig. 5.— The rest frame, dereddened continuum energy distribution of IRAS20051-1117. Note that the apertures used to derive fluxes in the various bands do not have the same size (see text for details).